Thermo-responsive Supramolecular Chemotherapy by "V"-shape Armed β-Cyclodextrin Star Polymer to Overcome Drug Resistance

Xiaoshan Fan[†], Hongwei Cheng[†], Xiaoyuan Wang, Enyi Ye, Xian Jun Loh, Yun-Long Wu, Zibiao Li**

Dr. X. Fan,
Collaborative Innovation Center of Henan Province for Green Manufacturing of Fine Chemicals, Key Laboratory of Green Chemical Media and Reactions, Ministry of Education, School of Chemistry and Chemical Engineering, Henan Normal University, Xinxiang, 453007, China.

H. Cheng, X. Wang, Prof. Y.-L. Wu,
Fujian Provincial Key Laboratory of Innovative Drug Target Research and State Key Laboratory of Cellular Stress Biology, School of Pharmaceutical Sciences, Xiamen University, Xiamen 361102, China.
E-mail: wuyl@xmu.edu.cn

Dr. E. Ye, Prof. X. J. Loh, Dr. Z. Li
Institute of Materials Research and Engineering, A*STAR (Agency for Science, Technology and Research); 2 Fusionopolis Way, Innovis, #08-03, Singapore 138634, Singapore.
E-mail: lizb@imre.a-star.edu.sg

[†] Both these authors made an equal contribution to this work.

Keywords: supramolecular chemotherapy, drug resistance, host-guest, thermo-sensitive

Abstract

Pump mediated drug efflux is the key reason to result in the failure of chemotherapy. Herein, a novel star polymer β-CD-*g*-(PEG-*v*-PNIPAAm)$_7$ consisting of a β-CD core, grafted with thermo-responsive poly(N-isopropylacrylamide) (PNIPAAm) and biocompatible poly(ethylene glycol) (PEG) in the multiple "V"-shaped arms is designed through the combination of esterification, "*Click*" chemistry and Reversible Addition Fragmentation Chain Transfer (RAFT), and further fabricated into supramolecular nanocarriers for drug resistant cancer therapy. With rational design of the unique architecture, β-CD-*g*-(PEG-*v*-PNIPAAm)$_7$ star polymer could encapsulate chemotherapeutics between β-cyclodextrin host cavity and guest anti-cancer drug *via* inclusion complex in high efficiency. Furthermore, the temperature induced chain association of PNIPAAm segment anchored in the junction point of the "V"-shaped arms could facilitate the inclusion complex to form into nanosized supramolecular formation at 37 °C, whereas the presence of PEG impart great stability to the self-assemblies. When incubated with MDR-1 (P-glycoprotein) membrane pump regulated drug resistant tumor cells, much higher and faster cellular uptake of the supramolecular nanoparticles were detected at 37 °C, and the enhanced intracellular retention of drugs could lead to significant growth inhibition of the cells. Further *in vivo* evaluation showed high therapeutic efficacy in suppressing drug resistant tumor growth in mice without a significant impact on the normal functions of main organs. This work signifies that thermo-responsive supramolecular chemotherapy is promising in combating pump mediated drug resistance in both *in vitro* and *in vivo* models, which may be encouraging for the advanced drug delivery platform design to overcome drug resistant cancer.

1. Introduction

Drug resistance, referring to the failure of drug effectiveness for the cancer patients receiving chemotherapeutics, becomes an undesired obstacle for successful chemotherapy.[1-4] Many clinical trials have reported the drug resistance of malignant with treatments of most popular chemotherapy drugs such as paclitaxel (PTX), doxorubicin (DOX), 5-fluorouracil, *etc*.[5, 6] Even worse, patients with drug resistance have to seek alternative chemotherapeutics or combination of multiple drugs and genes, which greatly impair the patient compliance and make the treatment more difficult.[7] As a typical example, PTX, one of the most effective anticancer therapeutics originated from Pacific yew, has been popularly utilized for treatments of liver, ovarian, lung, or breast cancers.[8-11] The tumor growth inhibition activity of PTX lies on its ability of tubulin β-subunit binding,[12, 13] which results in formation of polymerized microtubules and effectively inhibit mitosis at G2 phase before induction of cancer cell death.[14, 15] However, PTX could cause undesired drug resistance mainly in term of drug efflux increase.[16, 17] Drug efflux increase is heavily relied on the cancer cell's membrane pump resistance, which is mediated by MDR-1 protein. Interestingly, nanoparticle-based PTX delivery system holds great promise to overcome pump resistance by enhanced cellular uptake and increasing the PTX retention inside cancer cells.[18] However, the application of "nano" strategy in MDR-1 associated drug resistance is still worthy of further investigation.

Cyclodextrins (CDs) are a series of cyclic oligosaccharides, which are able to form supramolecular inclusion complexes with many drugs with suitable sizes by taking the advantages of their hydrophobic interior.[19, 20] Due to their aqueous solubility and low toxicity or immunity, CDs have been utilized to improve the solubility or stability of various chemotherapeutics.[21] As a typical, β-CD, composed of 7 D(+)-glucose units by

α-1,4-linkages, as well as its derivatives could enhance the solubility of hydrophobic paclitaxel (PTX) by forming inclusion complex in a 1:1 PTX/β-CD molecular ratio.[22, 23] Furthermore, DOX, as another popular chemotherapeutics, could also form complex with β-CD derivatives in a 1:2 DOX/β-CD molecular ratio for enhanced stability and bioavailability, indicating the importance of CDs in pharmaceutics.[24] Thanks to the unique drug encapsulation ability, CD as well as its derivatives have been successfully utilized in pharmaceutical carriers. As a typical examples, Xu et al. has conjugated ethanolamine-functionalized poly(glycidyl methacrylate) to β-CD and proved it to be an efficient gene carrier.[25, 26] To be mentioned, we also reported a series of star-shaped polymers consisting of a beta-cyclodextrin (β-CD) core and various functional components in the shell for enhanced therapeutic deliveries.[19, 27-30] For example, the co-delivery of anti-cancer drug and Nur77 gene in polyethyleneimine (PEI) grafted β-CD cationic supramolecular nanocarrier was successfully demonstrated to combat Bcl-2 mediated non-pump drug resistance.[28] However, in pump resistant cancers, the chemotherapeutic molecules were undesirably pumped outside the cell membrane, which requires more efficient pharmaceutical carriers to overcome the drug resistance.[31-34]

In this study, we constructed a novel temperature sensitive β-CD star polymer grafted with poly(N-isopropylacrylamide) (PNIPAAm) and biocompatible poly(ethylene glycol) (PEG) in the "V"-shaped arms (β-CD-*g*-(PEG-*v*-PNIPAAm)$_7$). The resultant start polymer could retain excellent drug-loading capacity below the lower critical solution temperature (LCST) due to the aqueous solubility of PNIPAAm and PEG arms. Furthermore, the increase of environment temperature to body temperature (37 °C, above LCST) would lead to the supramolecular formation of polymer/drug inclusion complex nanoparticles, which facilitated cellular endocytosis and inhibited the

membrane pump mediated drug resistance, as shown in **Scheme 1**. To the best of our knowledge, this is the first report of utilizing CD based star polymer with temperature sensitive nanoparticle formation ability for combating cancer drug resistance.

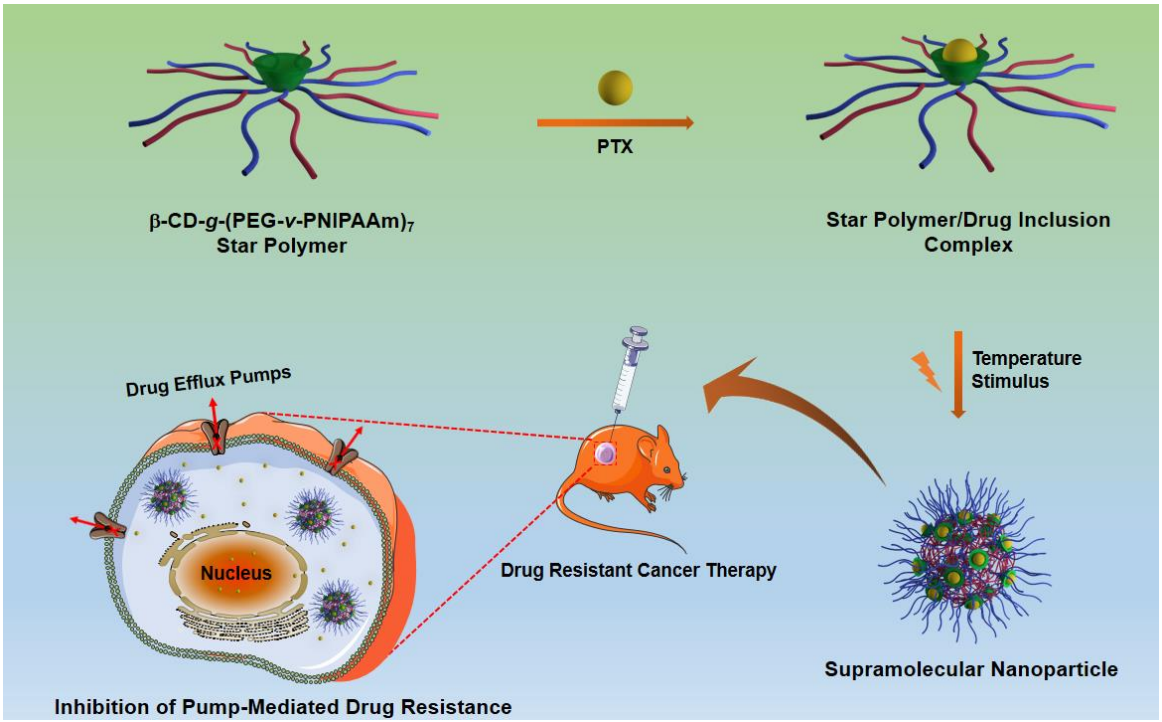

Scheme 1. Scheme illustration of star polymer β-CD-*g*-(PEG-*v*-PNIPAAm)$_7$ and its inclusion complex with chemotherapeutic PTX. The temperature induced supramolecular nanoparticle formation from the star polymer/drug inclusion complex show enhanced therapeutic efficiency towards the drug resistant cancer therapy.

2. Experimental

2.1 Materials

β-cyclodextrin (β-CD, Alladin) was dried at 80 °C under reduced pressure overnight prior to use. N-isopropylacrylamide (NIPAAm) (Acros Organics) was purified by recrystallization from n-hexane. Methoxy poly(ethylene glycol) (M_n = 2000 g/mol) was purchased from Sigma and purified by passing through a column with neutral alumina oxide to remove inhibitor. 2,2-Azoisobutyronitrile (AIBN) was purified by recrystallization from methanol. Dioxane was

dried by refluxing with the fresh sodium-benzophenone complex under N_2 and distilled before use. Dicyclohexylcarbodiimide (DCC, Alladin, 97%) and 4-(dimethylamino)pyridine (DMAP, Alladin, 98%) were used as received. The chain transfer agent (CTA) S-1-dodecyl-S′-(α,α'-dimethyl-α"-aceticacid) trithiocarbonae (DDAT) was synthesized according to previous method.[35] DMEM and RPMI1640 medium were purchased from Life Technology; TurboFect transfection reagent (Fermentas), SuperScript Reverse Transcriptase (Invitrogen) from Thermo Fisher Scientific; MDR1 antibody (22336-1-AP) was provided by Proteintech technology; immuno-histochemistry detection reagent (8114S) from Cell Signaling Technology (CST); 4,6-Diamidino-2-phenylindole (DAPI), [3-(4,5-dimethythiazol-2-yl)-2,5-diphenyl tetrazolium bromide] (MTT), doxorubicin, paclitaxel, puromycin from Sigma; Trizol reagent, PCR mixture regent and Gelred dye provided by Yeasen Biotech. The primers were synthesized by Sangon Biotech.

2.2 Synthesis of β-CD-(alkyne)$_7$ (Scheme 2)

Dried β-CD (0.302 g, 0.266 mmol) and 3-butynoxy carbonyl propionic acid (BCPA) (0.391 g, 2.300 mmol) were dissolved in 5 mL of anhydrous N,N-dimethylacetamide under stirring. As all of the substances were completely dissolved, 1-[3-dimethylamino)propyl]-3-ethylcarbodiimide (EDC·HCl) (0.439 g, 2.300 mmol) and a catalytic amount of amount of 4-(dimethylamino) pyridine (DMAP) were successively charged into the reaction flask under nitrogen flow. Then, the reaction mixture was stirred overnight at room temperature. The reaction solution was diluted with dichloromethane then washed with $NaHCO_3$ solution and deionized water successively. The organic phase was collected and dried with $MgSO_4$. After concentrated on a rotary evaporator, the residue was precipitated in cold diethyl ether to provide the targeted product.

2.3 Synthesis of α, α'-azide, CTA-PEG (PEG-N_3(CTA))

α, α'-azide, CTA-PEG (PEG-N_3(CTA)) was synthesized from the successive reactions of PEG-OH with epichlorohydrin, sodium azide and DDTA, as shown in Scheme S1. In this method, α, α'-azide, hydroxyl-PEG (PEG-N_3(OH)) was firstly synthesized, followed by the coupling reaction with DDTA to produce PEG-N_3(CTA).[27] In brief, PEG-N_3(OH) (1.059 g, 0.505 mmol) and DDAT (0.279 g, 0.764 mmol) were dissolved in dried CH_2Cl_2 and stirred until the solution became clear. Then, EDC (0.143 g, 0.748 mmol) and a catalytic amount of DMAP was added under nitrogen atmosphere. After 24 h reaction at room temperature, the product was collected by precipitation/dissolution in ethyl ether/dichloromethane twice.

2.4 Synthesis of star polymer β-CD-((CTA)PEG)$_7$ *via* "*Click*" reaction (Scheme 2)

To a Schlenk flask with 3 mL anhydrous DMF, 7-alkyne-β-CD (0.102 g, 0.044 mmol), mPEG-N_3(CTA) (0.826 g, 0.338 mmol) and PMDETA (70 μL, 0.338 mmol) were added. The system was degassed by nitrogen bubbling for 30 min. Then, CuBr (0.048 g, 0.338 mmol) was added followed by nitrogen bubbling for another 5 min. The reaction was kept at room temperature for 36 h under continous stir. The synthesized star polymer β-CD-((CTA)PEG)$_7$ was dialyzed against deionized water in dialysis tube (MWCO: 3500). The final product was collected by lyophilization.

2.5 Synthesis of thermosensitive star polymer β-CD-*g*-(PEG-*v*-PNIPAAm)$_7$ with "V"-shaped arms (Scheme 2)

β-CD-((CTA)PEG)$_7$ (0.103 g, 5.323×10^{-3} mmol), NIPAM (0.299 g, 2.646 mmol), AIBN (0.007 g, 0.043 mmol) and 4 mL anhydrous dioxane were charged into a Schlenk tube. After all of the substances were completely dissolved, the solution was degassed by nitrogen bubbling for 20 min. Then, the sealed flask was immersed into an oil bath preheated to 70 °C to start the

polymerization. After 24 h, the reaction was terminated by cooling down to room temperature and the reaction solution was precipitated in cold ethyl ether twice to produce the designed thermosensitive star polymer β-CD-*g*-(PEG-*v*-PNIPAAm)$_7$.

2.6 Overexpression of MDR1 in HepG2 and H460 cancer cells

The full length of MDR1 was cloned to the XbaI/BamHI site of pCDH vector to produced lentiviral particles of MDR1, and the sequence of primers as listed. The forward primer: 5'-GCT CTA GAA TGG ATC TTG AAG GGG ACC GCA ATG-3', the reverse primer: 5'- CGG GAT CCT CAC TGG CG CT TTG TTC CAG CCT-3'. Overexpression lentivirus particles of MDR1 was harvested after HEK293T transfected with MDR1 lentiviral plasmid, and then infected into HepG2 and NIH-H460 cells. After 72 h transfection, and then treated with puromycin (5 μg/mL final concentration) in complete medium for 2-3 days to select stably expressing MDR1 cell lines and verify availability of stable expression cell lines using RT-PCR and Western blotting. The sequence of primers for RT-PCR as followed: MDR1 (forward: 5'-CGA CAG GAG ATA GGC TGG TT -3'; reverse: 5'- AGA ACA GGA CTG ATG GCC AA -3'), GAPDH (forward: 5'-AGG TCG GAG TCA ACG GAT TT -3'; reverse: 5'- ATC TCG CTC CTG GAA GAT GG-3').

2.7 Preparation of supramolecular inclusion complex between thermo-sensitive star polymer β-CD-*g*-(PEG-*v*-PNIPAAm)$_7$ and chemotherapeutics

The general process for preparation of polyplex between β-CD-*g*-(PEG-*v*-PNIPAAm)$_7$ and doxorubicin or paclitaxel, as described below. A solution of paclitaxel or doxorubicin (1 mg) in ethanol (2 mL) was respectively added a solution of β-CD-*g*-(PEG-*v*-PNIPAAm)$_7$ (10 mg) dissolved in deionized water (5 mL), and stirred at room temperature in the dark for 4 days. After incubation, the complex was harvested and centrifuged to dislodge the insoluble

compound, and the solvent was lyophilized overnight by freeze drier. Then subjected to calculate the yield with NMR.

2.8 Cell culture

HepG2 liver cancer cells, HEK293T embryonic kidney cells and NIH-H460 lung cancer cell were obtained from American Type Culture Collection (ATCC). HepG2 and HEK293T were cultured in Dulbecco's Modified Eagle's Medium and NIH-H460 was cultured in RPMI 1640 Medium, supplemented with 10% fetal bovine serum (FBS), 100U/mL penicillin and 100 μg/mL streptomycin in humidified 5% CO2 at 37 °C incubator. HepG2-MDR1, H460-MDR1 and the respective control were maintained with 1 μg/mL puromycin for stable selection.

2.9 Cell viability assay

[3-(4,5-dimethythiazol-2-yl)-2,5-diphenyl tetrazolium bromide] (MTT) method was used to test cell viability *in vitro*. MDR1-overexpression and the respective control cells were seeded at the density of 5×10^3 cells per well. After 24 h incubation, treatment with indicated compound for 24 h, and then added 10 μL of MTT (5 mg/mL) per well. After incubated 4 h, and dissolved crystals with DMSO. With shaking 10 min, and detected the absorbance ratio at 492 nm with Microplate Reader (Thermo). The mean OD values were calculated and cell viability curves were conducted. All experiments were conducted with six repetitions and averaged.

2.10 Confocal assay

HepG2/MDR1 cells were seeded on glass coverslips in 24-well plates (5000 cells/ per coverslip). Treatment with β-CD-*g*-(PEG-*v*-PNIPAAm)$_7$/Dox with indicated time at 37 °C or

25 °C. And cells were fixated with 4% paraformaldehyde for 10 min and then permeabilized with 0.1% Triton X-100 and 0.1M Glycine for 20 min on ice. Cells were stained DAPI (4',6'-diamidino-2-phenylindole) to visualize nucleus. The images were taken under a LSM-510 confocal laser scanning microscope system.

2.11 Animal *in vivo* study

Nude mice (BALB/c, SPF grade, 17 – 19 g, 5 – 6 weeks old) were injected subcutaneously with 100 μL HepG2-MDR1 cells (2×10^6cells per mouse), After 4 days of transplantation, mice were injected intratumorally once every 2 days with β-CD-*g*-(PEG-*v*-PNIPAAm)$_7$/PTX (C_{PTX} = 5 mg/kg), paclitaxel (C_{PTX} = 5 mg/kg) or vehicle control. Body weight and tumor sizes were measured every 2 days. After 12-days drug treatment, mice were sacrificed and the tumors were removed for next assessments. Tumor volumes were calculated using the equation: V (cm^3) = width^2 (cm^2) × length (cm)/2. The animal experiment was approved by the Animal Care and Use Committee of Xiamen University and animal experiments were performed in accordance with the National Institutes of Health guideline.

2.12 Hematoxylin and eosin staining and immunohistochemistry staining

The tumors and other organ tissues were removed for histological analysis after mice sacrificed. Paraffin sections were made in standard protocol with the thickness of 5 μm. The sections were stained with hematoxylin and eosin according to standard method. The expression of cleavage-caspase 3 was detected with cleavage-caspase 3 antibody, and the sections were co-stained with hematoxylin to visualize nuclear. All sections were observed by Olympus biomicroscope.

2.13 Western blotting

The cell lysates, from cells with treatment of RPIA lysis buffer (50 mM Tris (pH 7.4), 1% TritonX-100, 150 mM NaCl, 0.1% SDS, and 1% sodium deoxycholate), were electrophoresed on 8% SDS-PAGE for protein separation, before transfection to PVDF membranes. After that, membranes were further incubated with MDR1 primary antibodies and horseradish peroxidase conjugated secondary antibodies. The immune-reactive bands were detected by ECL system.

2.14 Statistical analysis

Cell viability, tumor volume, and tumor weight in experiments were calculated as by expressing the mean ± standard deviation. Statistics analysis was performed by Origin 8 using two-tailed student's t tests to compare the statistical significance. * p-values < 0.05 was considered to be significant.

3. Results and Discussion

3.1 Synthesis and characterization of thermo-sensitive star polymer with "V"-shaped arms β-CD-*g*-(PEG-*v*-PNIPAAm)$_7$

The designed synthetic route to the star-like copolymer β-CD-*g*-(PEG-*v*-PNIPAAm)$_7$ consisting of a β-CD core and multiple “V”-shaped arms PEG-*v*-PNIPAAm is depicted in **Scheme 2**. A star-shaped polymer has a higher segment density within the distance of its radius of gyration than a homologous linear polymer does under the same condition. Therefore, the excluded volume effects are more pronounced in star-shaped polymers.[36] By designing the arm chains into “V”-shaped structure, the excluded volume effects are expected to be more profound than regular star-shaped polymers, and this would have a significant effect on the overall conformation of the polymer chain in solution. During the synthesis, the alkyne groups were firstly introduced onto the β-CD core *via* EDC/DMAP catalyzed esterification between β-CD and BCPA to produce β-CD-(alkyne)$_7$. The alkyne groups were mainly grafted onto the 6-

positioned primary hydroxyl groups on the upper rim of the β-CD due to the higher reactivity than that of secondary ones on the lower rim of the β-CD. Therefore, the graft number of alkynes on β-CD was finely controlled by the feed ratio of β-CD and 3-butynoxy carbonyl propionic acid (BCPA). After that, the pre-prepared PEG-N_3(CTA) (**Scheme S1 and Figure S1**) was "grafted onto" the multifunctional core β-CD-(alkyne)$_7$ by "*Click*" reaction to afford star polymer β-CD-*g*-((CTA)PEG)$_7$, where the reactive CTA groups were anchored at the junction point of the star polymer (**Scheme 2**). Finally, PNIPAAm arms were grafted from β-CD-*g*-((CTA)PEG)$_7$ *via* "graft from" approach to give the desired β-CD-*g*-(PEG-*v*-PNIPAAm)$_7$. The presence of β-CD in the star polymer β-CD-*g*-(PEG-*v*-PNIPAAm)$_7$ can be further used to encapsulate therapeutic drugs by host-guest interaction.

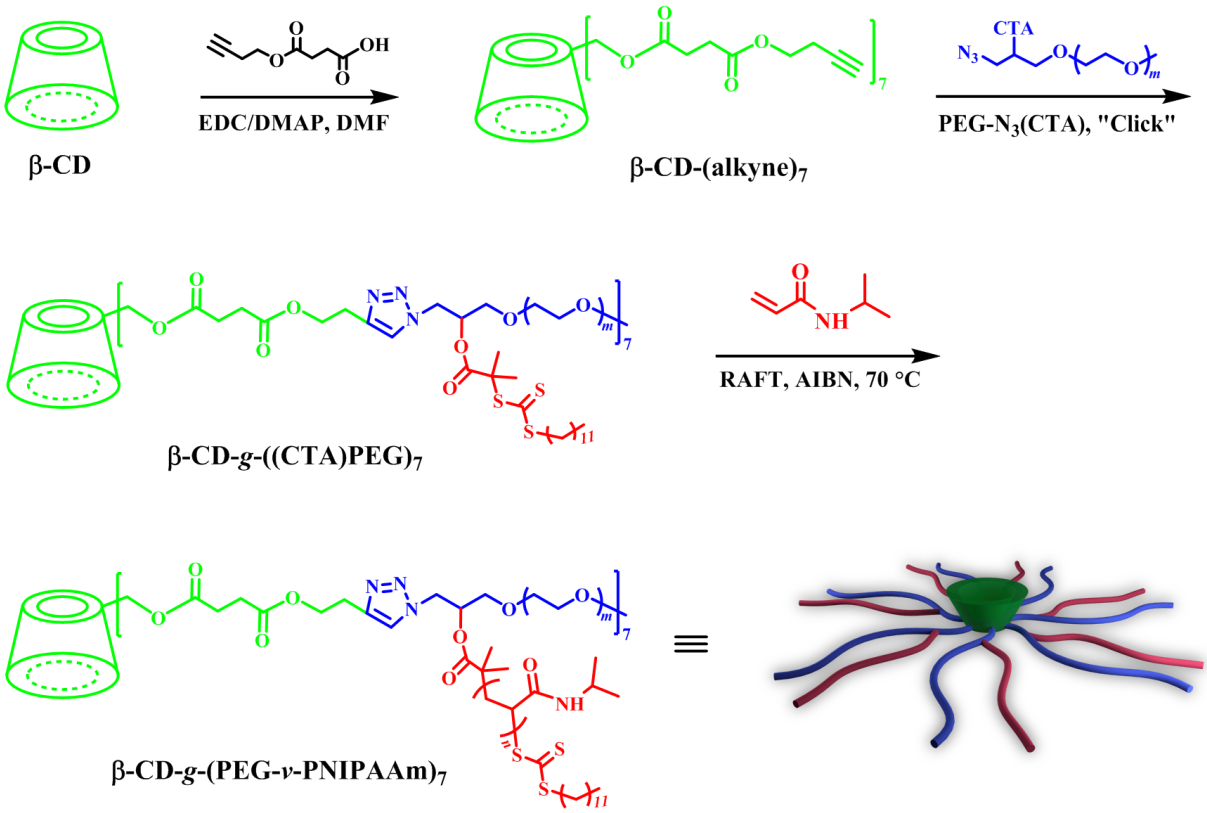

Scheme 2. Synthetic route and schematic illustration of thermo-sensitive star polymer β-CD-*g*-(PEG-*v*-PNIPAAm)$_7$ with "V"-shaped arms.

The star-like β-CD-*g*-(PEG-*v*-PNIPAAm)$_7$ polymer and its intermediates were characterized by ^{1}H NMR and GPC techniques. As shown in **Figure 1A**, the signals corresponding to β-CD core and the BCPA moieties were observed clearly in β-CD-(alkyne)$_7$. The degree of substitution (DS) was calculated by the integration ratio of the signals for the methyl protons (b,d) at 2.52 and 2.66 ppm of the BCPA group to those of the 1-postioned protons (-C(1)H) of β-CD at 4.96 ppm. From this method, the average number of CTA grafted on per CD molecule in β-CD-(alkyne)$_7$ was calculated to be 7. **Figure 1B** shows the typical ^{1}H NMR spectrum of β-CD-*g*-((CTA)PEG)$_7$, in which the characteristic signals (b) at 3.65 ~ 3.89 ppm ascribed to the PEG arms are clearly observed. Based on the integration ratio between signals (a) and (e), the graft degree of PEG arms on each β-CD-(alkyne)$_7$ was calculated to be approximate 7, indicating the high efficiency of *"Click"* reaction in macromolecular construction. In addition, the GPC trace of β-CD-*g*-((CTA)PEG)$_7$ diaplayed unimodal distribution as presented in **Figure 2A**. These results showed that star-like β-CD-*g*-((CTA)PEG)$_7$ polymer with attached PEG arms was successfully synthesized. The obtained β-CD-*g*-((CTA)PEG)$_7$ was further used as macro chain transfer agent to initiate the polymerization of NIPAAm monomers *via* RAFT to yield the designed thermosensitive star polymer β-CD-*g*-(PEG-*v*-PNIPAAm)$_7$ with "V"-shaped arms. For the ^{1}H NMR spectrum shown in **Figure 1C**, the signals belong to the methyl protons (δ 1.14 ppm), methylidyne protons adjacent to the carbonyl group (δ 1.78 ppm), as well as the methylidene protons linked to the amine moiety (δ 3.95 ppm) of PNIPAAm arms were detected, as reported previously.[37] Based on the integeration ratio of the signal (f) of PEG to signal (l) of PNIPAAm, the degree of polymerization of PNIPAAm was determined to be 45 (Mw: 5,140 g/mol). In addition, the typical peak assignments associated with PEG were also observed in β-CD-*g*-(PEG-*v*-PNIPAAm)$_7$ spectrum, confirming the "V"-shaped architecture in the arms of the star polymer. More importantly, the GPC trace of β-CD-*g*-(PEG-*v*-PNIPAAm)$_7$ also exhibited a monomodal characteristic and shifted toward the higher molecular weight region in

comparison with its prepolymer β-CD-*g*-((CTA)PEG)$_7$, further confirming the succesful synthesis of the desired star polymer.

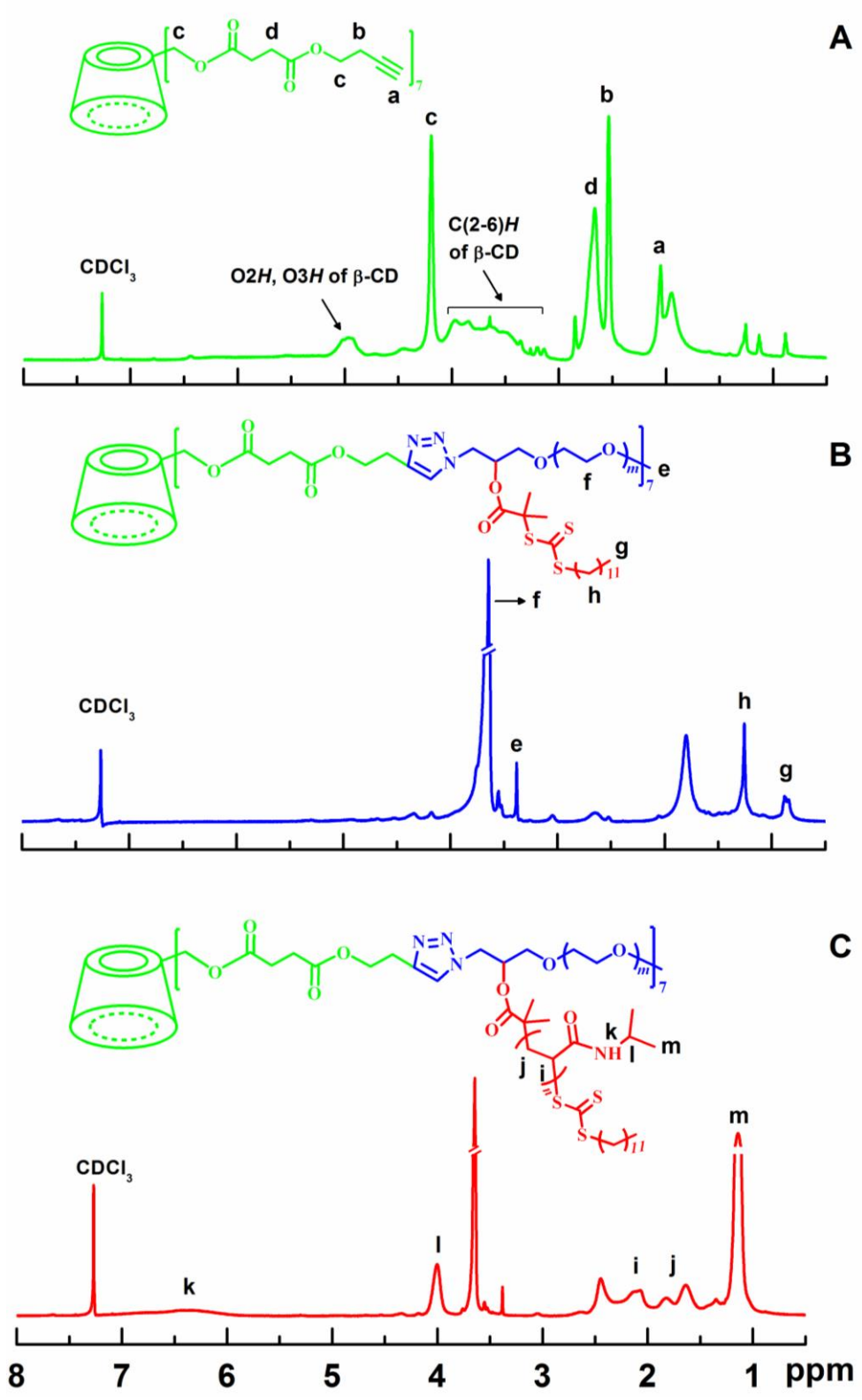

Figure 1. ^{1}H NMR spectra of (A) β-CD-(alkyne)$_7$, (B) β-CD-*g*-((CTA)PEG)$_7$ and (C) of β-CD-*g*-(PEG-*v*-PNIPAAm)$_7$ in $CDCl_3$. The peak assignments in (A) are also applicable to (B) and (C).

3.2 Formation of supramolecular inclusion complex

β-CD-*g*-(PEG-*v*-PNIPAAm)$_7$ star copolymer was dissolved with paclitaxel (PTX) or doxorubicin (DOX) in 2:1 molar ratio in a mixture solution of water/ethanol (1:1, v/v) for 4 days in the dark. PTX or DOX molecules were encapsulated into the hydrophobic β-CD core of these compounds. The ^{1}H NMR spectroscopy indicated successful inclusion complex formation between β-CD-*g*-(PEG-*v*-PNIPAAm)$_7$ and PTX, as shown in **Figure 2C**. Due to the poor aqueous solubility of PTX, there was no proton peaks observed from NMR spectrum by using D_2O as solvent. And the appearance of phenyl signals (δ 7.2-8.2) from β-CD-*g*-(PEG-*v*-PNIPAAm)$_7$/PTX complex strongly provided the evidence of successful complexation between β-CD-*g*-(PEG-*v*-PNIPAAm)$_7$ and PTX.[38] It could also be calculated that the ratio of β-CD-*g*-(PEG-*v*-PNIPAAm)$_7$ to encapsulated PTX was close to 1:1, which indicated a 2.9 wt% drug loading amount and 93% encapsulation efficiency, which out-performed 1.0 wt % loading level and 83% of encapsulation efficiency of PTX in the β-CD-(N_{32})$_4$/PTX inclusion complexes previously reported.[39] Considering the low encapsulation efficiency of PTX by β-CD, Me-β-CD or HP-β-CD in previous reports, the presence of PEG-*v*-PNIPAAm in the designed β-CD-*g*-(PEG-*v*-PNIPAAm)$_7$ showed significantly improved solubilization of PTX due to its hydrophilic PEG and PNIPAAm which could facilitate the inclusion complex formation.[39] As for DOX, the inclusion complex formation was investigated by fluorescence emission measurements of DOX in the presence of β-CD-*g*-(PEG-*v*-PNIPAAm)$_7$ at various concentrations. As shown in **Figure 2D**, with increasing amount

of β-CD-*g*-(PEG-*v*-PNIPAAm)$_7$, the typical fluorescence intensity of DOX at 600 nm decreases sharply, indicating the enhanced host-guest interaction between the two molecules, as reported previously.[40-42]

The thermo-responsive behavior of β-CD-*g*-(PEG-*v*-PNIPAAm)$_7$ star polymer was investigated by the optical transmittance change in the test solutions as a function of temperature.[27] PNIPAAm homopolymer exhibits a temperature-sensitive phase transition in the temperature range of 32 – 34 °C. This temperature is known as the cloud point temperature and has been used to determine the lower critical solution temperature (LCST).[37] As shown in **Figure 2B**, the LCST of β-CD-*g*-(PEG-*v*-PNIPAAm)$_7$ star polymer is 34.8 °C. Below this temperature, β-CD-*g*-(PEG-*v*-PNIPAAm)$_7$ and its inclusion complex with chemotherapeutic drugs presented as single molecule states (**Table S1**). However, when temperature was increased to 37 °C (above LCST), the PNIPAAm chains underwent phase transition and the intermolecular association could facilitate β-CD-*g*-(PEG-*v*-PNIPAAm)$_7$ and its inclusion complex to form supramolecular nanoparticles. As presented in **Figure 2 (F-G)**, the sizes of β-CD-*g*-(PEG-*v*-PNIPAAm)$_7$/drug supramolecular assemblies determined by DLS display a unimodal distribution with an average hydrodynamic diameter of 190 – 230 nm. The supramolecular nanoparticles were further characterized by TEM visualization. Representative images of the as-formed supramolecular nanoparticles show a spherical morphology and the sizes viewed by TEM are in good agreement with the results measured on DLS (**Figure 2 F-G**). These results indicate that the supramolecular assemblies of β-CD-*g*-(PEG-*v*-PNIPAAm)$_7$/drugs inclusion complex at 37 °C could lead to the formation of compact nanoparticles, which can be effectively endocytosed by cells. As nanoparticles with diameter between 100 – 200 nm were beneficial to enhanced

permeability and retention (EPR) effect, these PNIPAAm-β-CD-POEGA/drug complex nanoparticles might be attractive for future cancer therapy.[43, 44]

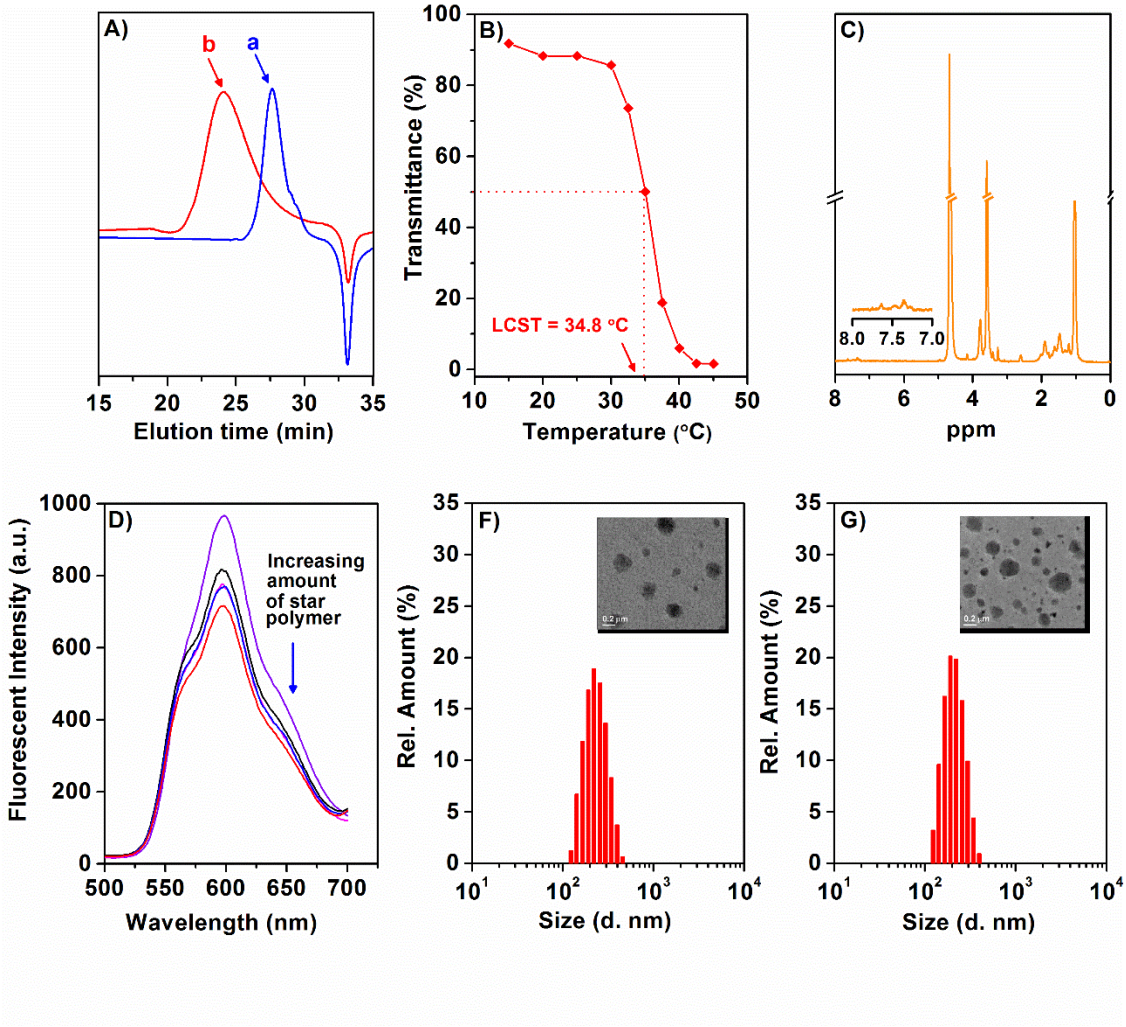

Figure 2. Characterizations of of β-CD-*g*-(PEG-*v*-PNIPAAm)$_7$ star polymer and its supramolecular inclusion complex with chemotherapeutic drugs. (A) GPC traces of (a) β-CD-*g*-((CTA)PEG)$_7$ and (b) β-CD-*g*-(PEG-*v*-PNIPAAm)$_7$ star polymers. (B) Thermo-responsive behavior of β-CD-*g*-(PEG-*v*-PNIPAAm)$_7$ star polymer aqueous solutions as a function of temperature. Polymer concentration at 2.0 mg/mL was used in the measurement. (C) ^{1}H NMR spectra of β-CD-*g*-(PEG-*v*-PNIPAAm)$_7$/PTX host-guest inclusion complex in D_2O. (D)

Fluorescence emission spectra of DOX in the presence of increasing amount of β-CD-*g*-(PEG-*v*-PNIPAAm)$_7$ star polymer. Particle size distribution of (F) β-CD-*g*-(PEG-*v*-PNIPAAm)$_7$/PTX and (G) β-CD-*g*-(PEG-*v*-PNIPAAm)$_7$/DOX supramolecular nanoparticles at 37 °C. The inset graphs show the particle morphologies recorded by TEM (scale bar: 200 nm)

3.3. Establishment of MDR1 drug resistant cancer cells

In order to construct MDR1 (P-glycoprotein) high expression cell lines as a model of drug resistant cancer cells, the MDR1 gene was connected to a lentivirus pCDH vector before transfection into the HepG2 liver cancer cells or H460 non-small lung cancer cells. MDR1 stable expression cells were obtained through screening by puromycin and then monocloned. The protein expression of the MDR1 were observed by western blot analysis, as shown in **Figure 3A**. The results showed that the protein levels of P-glycoprotein were elevated in both HepG2/MDR1 and H460/MDR1 cell lines.[45] Similarly, the mRNA levels of MDR1 in HepG2/MDR1 or H460/MDR1 cells were also significantly higher than that in the cells with transfection of a vector only, as shown in Figure 3B, indicating the successful establishment of MDR1 high expression cancer cell lines.[46]

To further evaluate the drug resistance ability of MDR1 high expression cancer cells, the cell viability of HepG2/MDR1 or H460/MDR1 cells, with the treatment of differently concentrated PTX or DOX, was evaluated by the MTT assay.[47] Interestingly, 5 – 60 nM of PTX could induce obvious cancer cell death in HepG2 or H460 cancer cells but their effects on HepG2/MDR1 or H460/MDR1 cells were significantly reduced, as shown in Figure 3C. The increase of half maximal inhibitory concentration (IC_{50}) values for PTX from 8.4 nM in HepG2 cells to 70 nM in HepG2/MDR1 cells or for DOX from 0.2 μM in HepG2 cells to 6.5 μM in HepG2/MDR1 cells (Table S2). Similarly, the IC_{50} values for PTX were also increased

from 10 nM in HepG2 cells to 36 nM in HepG2/MDR1 cells or for DOX from 0.2 μM in HepG2 cells to 3.3 μM in HepG2/MDR1 cells, indicating the chemotherapeutic resistance in MDR1 high expression cancer cells (**Table S2**).[48]

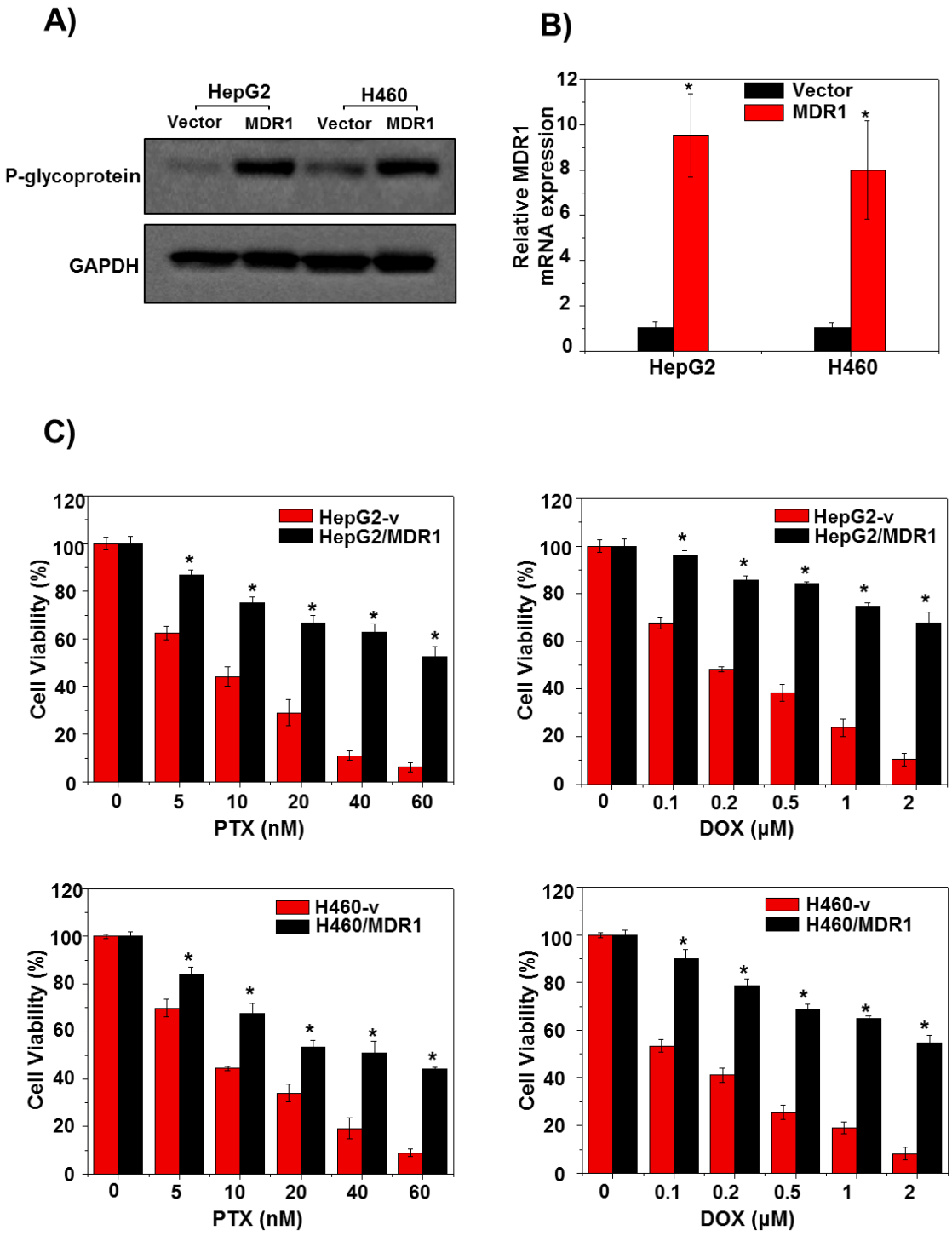

Figure 3. Establishment of drug resistant HepG2/MDR1 or H460/MDR1 cancer cell lines. (A) Western blotting to analyze the protein expression of P-glycoprotein in MDR1-overexpressing

or vector control HepG2 and H460 cells. (B) RT-PCR assay to examine the MDR1 mRNA expression in MDR1 overexpression HepG2/MDR1 and H460/MDR1 or vector control cell lines. (C) MTT assay was conducted to detect the cell viability of HepG2/MDR1, H460/MDR1 and vector control cell lines in increasing dose of PTX or Dox. Data represents in the form of mean ± standard derivatives. *$p < 0.05$, compared with the vector control cell line respectively, $n = 6$.

Interestingly, the above drug resistance could be reversed by the *in vitro* delivery of PTX or DOX in the form of β-CD-*g*-(PEG-*v*-PNIPAAm)$_7$/PTX or β-CD-*g*-(PEG-*v*-PNIPAAm)$_7$/DOX inclusion complex, as shown in **Figure 4**. In details, the IC_{50} value for PTX was 70 nM in drug resistant HepG2/MDR1 liver cancer cells or 36 nM in drug resistant H460/MDR1 lung cancer cells respectively, while its IC_{50} value was reduced to be 13 nM in HepG2/MDR1 and 6.3 nM in H460/MDR1 cells in the form of β-CD-*g*-(PEG-*v*-PNIPAAm)$_7$/PTX complex. Similarly, the IC_{50} values of DOX were reduced from 6.5 μM in HepG2/MDR1 cells and 3.3 μM in H460/MDR1 cells to below 0.2 μM in both cell lines, indicating the significant drug resistant cancer cell death rate increase by incorporating chemotherapeutics in rationally designed β-CD-*g*-(PEG-*v*-PNIPAAm)$_7$ carrier.

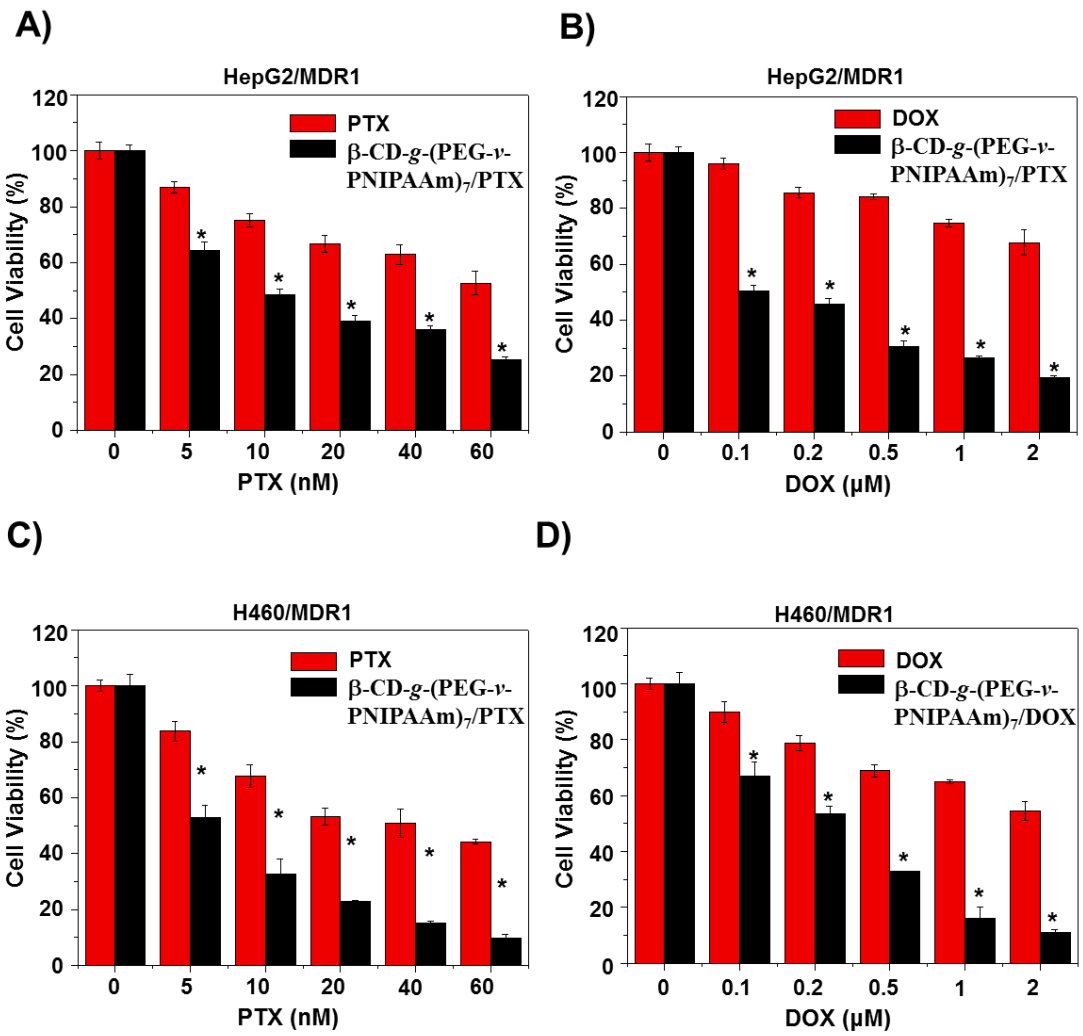

Figure 4. Cell viability assay to study of β-CD-*g*-(PEG-*v*-PNIPAAm)$_7$/drug supramolecular nanoparticles for reversing MDR1-related drug resistance. (A) Cell viability of HepG2/MDR1 and (C) H460/MDR1 after 24 h treatment with indicated doses of PTX supramolecular nanoparticles or equivalent PTX only. (B) Treatment with DOX supramolecular nanoparticles or equivalent Dox only in HepG2/MDR1 and (D) H460/MDR1 cell lines for 24 h. Data represents in the form of mean ± standard derivatives. *$p < 0.05$, with comparison to growth inhibition of PTX or DOX treatment only, n = 6.

3.4 Thermo-responsive cellular uptake of β-CD-*g*-(PEG-*v*-PNIPAAm)$_7$/drug supramolecular nanoparticles

In order to understand the possible of increased drug resistant cell growth inhibition by β-CD-*g*-(PEG-*v*-PNIPAAm)$_7$/drug supramolecular nanoparticles, fluorescent DOX was utilized as a model chemotherapeutics to study the *in vitro* cellular uptake behaviour, as shown in Figure 5. Experimental results showed that the cellular uptake of DOX was low due to the high expression of MDR1 proteins in HepG2/MDR1 cells.[39] Similar case was observed for β-CD-*g*-(PEG-*v*-PNIPAAm)$_7$/DOX sample at 25 °C within 24 h (**Figure 5**). Interestingly, much higher and faster cellular uptake of fluorescent DOX could be visualized at different time points at 37 °C, which was probably due to the supramolecular nanoparticle formation at temperature above LCST. The PNIPAAm chains became hydrophobic and its intermolecular associations promoted the drug-loaded star polymers to form supramolecular nanoparticle formation at body temperature. Together with PEGylation presented in the "V"-shaped arms, it favoured the cellular uptake of the inclusion complexes synergistically and thus enhanced drug delivery or increased drug retention time (**Figure 2 and 5**).

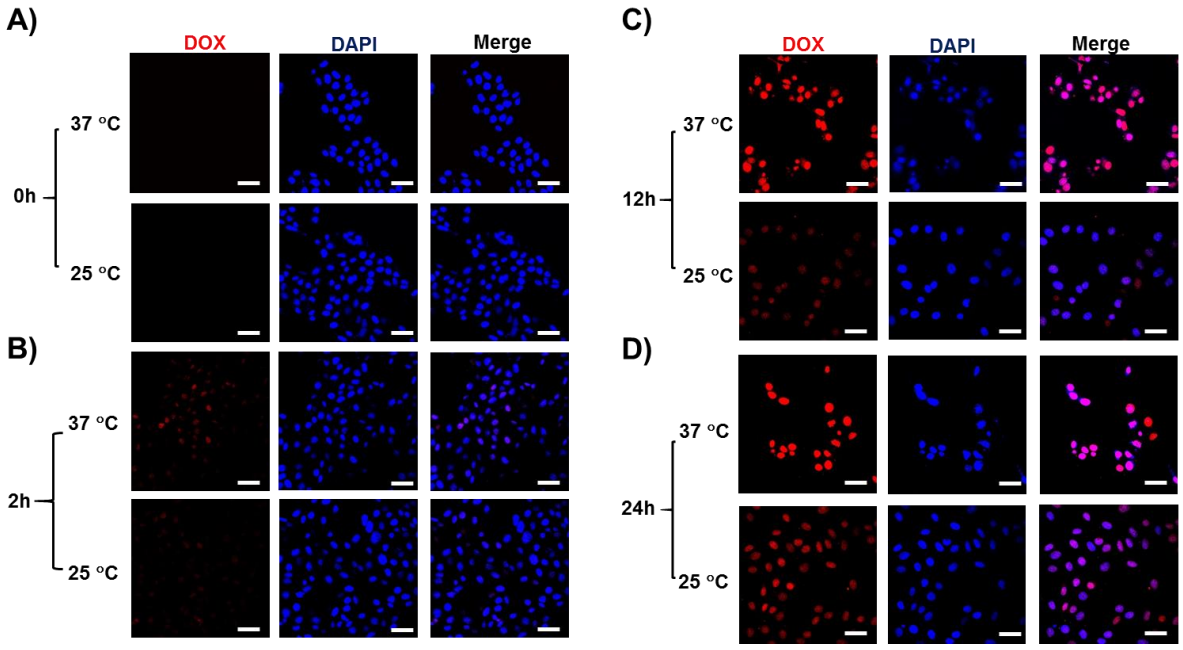

Figure 5. Confocal microscope images showing the thermo-responsive cellular uptake of β-CD-*g*-(PEG-*v*-PNIPAAm)$_7$/DOX supramolecular nanoparticles in drug resistant HepG2/MDR1 cells. The cells were plated in glass coverslips and cultured for 24 h, and then β-CD-g-(PEG-v-PNIPAAm)$_7$/Dox with indicated time at 37 °C or 25 °C. DAPI was used to stain the nucleus (Scale bar: 20 μm).

3.5 *In vitro* MDR1 drug resistant cancer cell growth inhibition

In order to investigate whether the increased cellular uptake or intracellular retention of drugs could lead to enhanced growth inhibition of drug resistant HepG2/MDR1 cancer cells. *In vitro* cytotoxicity of HepG2/MDR1 or H460/MDR1 cancer cells with treatment of β-CD-*g*-(PEG-*v*-PNIPAAm)$_7$/PTX and β-CD-*g*-(PEG-*v*-PNIPAAm)$_7$/DOX supramolecular nanoparticles were further evaluated by using the MTT viability assay at 25 °C and 37 °C, respectively. As shown in Figure 6 and Figure S2, the host star polymer β-CD-*g*-(PEG-*v*-PNIPAAm)$_7$ without drugs show very high cell viability at both cancer cells with or without high expression of MDR1 proteins. In addition, the HepG2/MDR1 and H460/MDR1 cell growth were significantly inhibited with the treatment of β-CD-*g*-(PEG-*v*-PNIPAAm)$_7$/drug supramolecular nanoparticles at 37 °C rather than the inclusion complex at 25 °C, indicating the importance of thermo-responsive properties of the star polymeric carrier (**Figure 6 and Figure S3**).

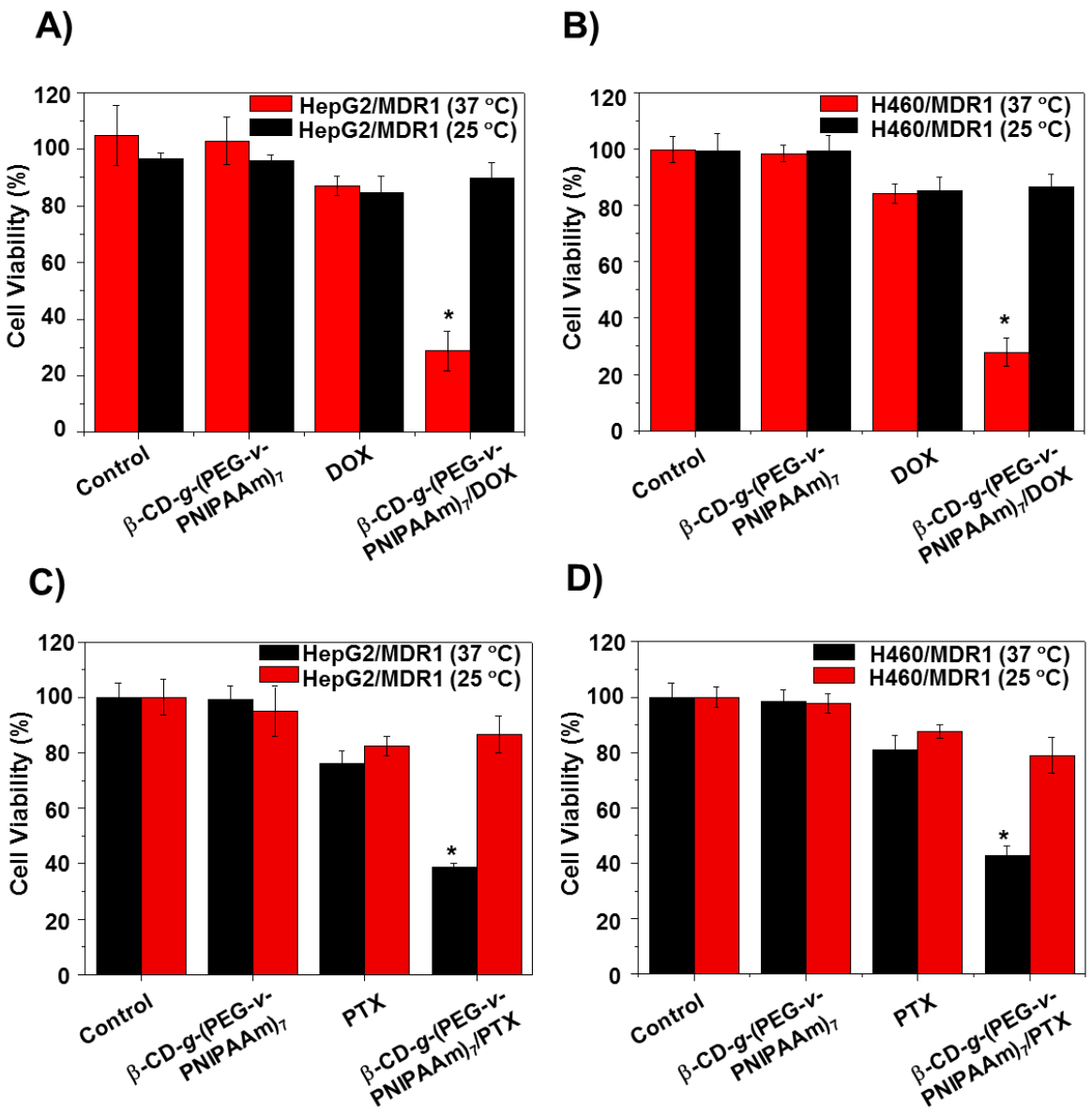

Figure 6. *In vitro* MDR1 drug resistant cancer cell growth inhibition by thermo-sensitive β-CD-*g*-(PEG-*v*-PNIPAAm)$_7$/drug supramolecular nanoparticles. Before treatment with indicated inclusion complex, cells were plated in 96-wells for culture at 37 °C. After 24 h culture, (A) HepG2/MDR1 or HepG2 vector control cells and (B) H460/MDR1 or H460 vector control cells with treatments of β-CD-*g*-(PEG-*v*-PNIPAAm)$_7$, DOX (0.5 μM) and β-CD-*g*-(PEG-*v*-PNIPAAm)$_7$/DOX inclusion complex at 37 °C or 25 °C for 24 h culture. (C-D) Drug resistant cancer cell growth inhibition by PTX (10 nM) as well as its supramolecular complex form of β-CD-*g*-(PEG-*v*-PNIPAAm)$_7$/PTX in (C) HepG2/MDR1 and (D) H460/MDR1 cells at different conditions. Data represents in the

form of mean ± standard derivatives. * $p < 0.05$ was considered as significant difference, n = 6.

3.6 *In vivo* drug resistant cancer therapy

To reveal whether the delivery of PTX by using the β-CD-*g*-(PEG-*v*-PNIPAAm)$_7$ could increase the *in vivo* therapeutic efficacy, the antitumor effect was further evaluated in mice bearing HepG2/MDR1 tumor xenografts. As shown in **Figure 7**, compared with the treatment of free chemotherapeutic PTX, β-CD-*g*-(PEG-*v*-PNIPAAm)$_7$/PTX supramolecular assemblies with the ability to form inclusion complexes with PTX for improved aqueous solubility and enhanced retention effects could significantly inhibit the growth of drug resistant HepG2/MDR1 tumor. In details, after 12 days, the final tumor size of the control saline group was 391 mm^3 ± 154 mm^3, indicating a large tumor growth. In the case of PTX, due to the utilization of the HepG2/MDR1 drug resistance tumor xenograft, the tumor size was 305 mm^3 ± 131 mm^3, indicating a low growth inhibition efficiency when free PTX was used. However, significant tumor growth inhibition in β-CD-*g*-(PEG-*v*-PNIPAAm)$_7$/PTX was detected, with a final volume of 84 mm^3 ± 69 mm^3 (**Figure 7A-C**). This is properly due to the successful enhanced retention of intracellular PTX after formation of supramolecular nanoparticles in the drug resistant tumor model. Similar to the observation of the volume of tumor shrinkage, the tumor weights were also significantly decreased after the 12 days therapy, decreasing to about 30% in comparison with the control saline group (**Figure 7D**), without a significant impact on the mice body weight measured at various time points to assess the health of the mice or the normal function of main organs (**Figure S4**).

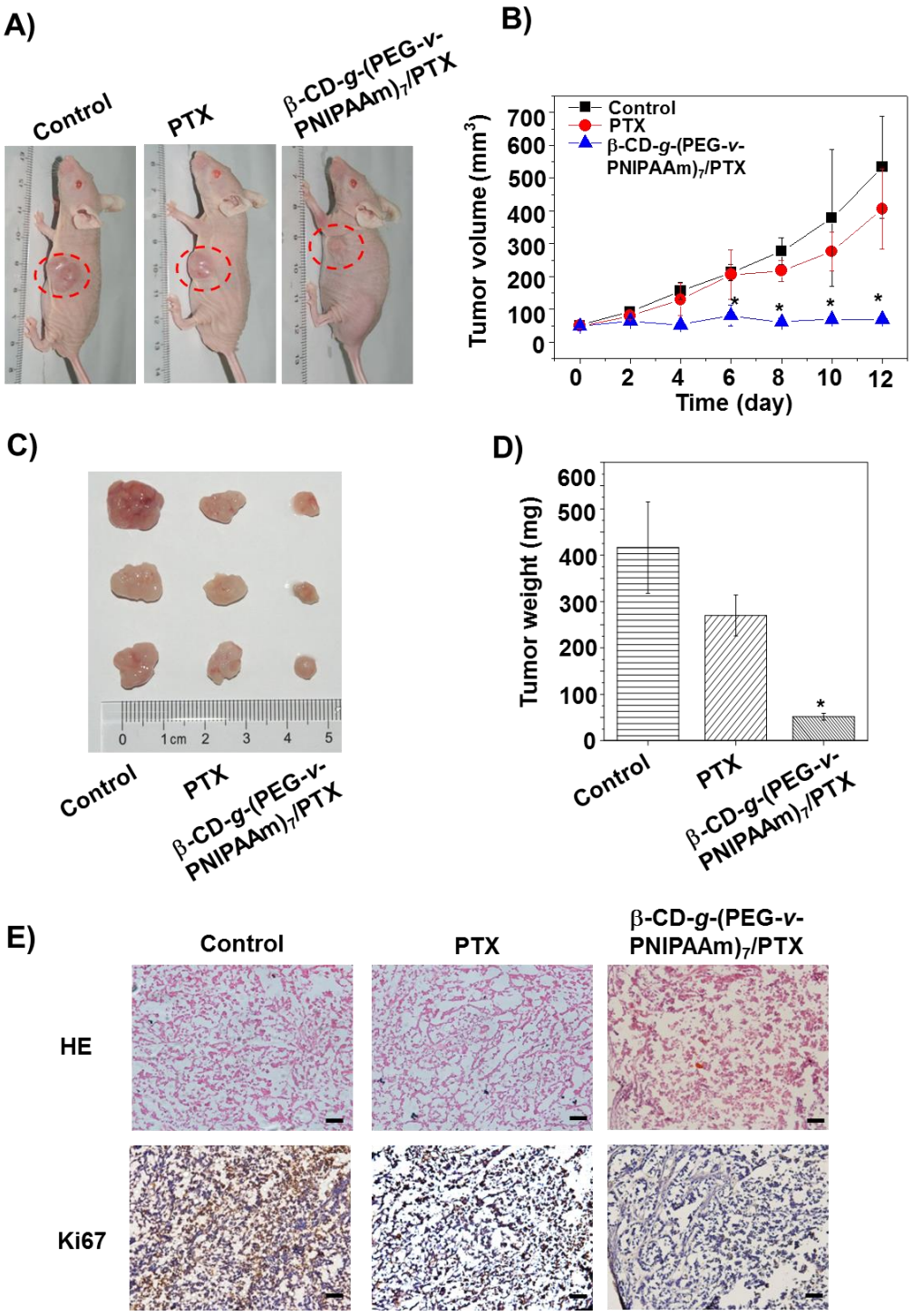

Figure 7. *In vivo* study of drug delivery by thermo-sensitive β-CD-*g*-(PEG-*v*-PNIPAAm)$_7$/drug supramolecular nanoparticles for potential drug resistant cancer therapy. (A) With the treatment of β-CD-*g*-(PEG-*v*-PNIPAAm)$_7$/PTX or PTX only after 12 days, the size of subcutaneous tumor was recorded by photograph. (B) Indicate a significant reduction in tumor volume between PTX-treated group and β-CD-*g*-(PEG-*v*-

PNIPAAm)$_7$/PTX. (C) Tumor images of HepG2/MDR1 xenograft and (D) tumor weight was calculated after 12 days indicated treatment. (E) Paraffin-embedded sections were subjected to immunohistochemical analysis with HE staining and Ki67 expression after indicated treatment for 12 days (Scale bar: 50 μm). Data represents in the form of mean ± standard derivatives. * $p<0.05$, in comparison with treatment of PTX only, n = 3.

After 12 days, the mice were sacrificed and subcutaneous tumors were isolated for HE staining and c-caspase3 protein expression analysis (**Figure 7E**). H&E staining results of representative tissue sections clearly showed that only a few apoptotic or necrotic regions were found in control or PTX only group, indicating their inefficiency in treating drug resistant tumors. However, the edge and the middle of tumors from the β-CD-*g*-(PEG-*v*-PNIPAAm)$_7$/PTX group showed an increased apoptosis or necrosis area, which might be due to the enhanced cellular uptake of PTX. More importantly, immunostaining of tissue sections showed that the administration of β-CD-*g*-(PEG-*v*-PNIPAAm)$_7$/PTX resulted in decreased expression of Ki67, one proliferation marker in the diagnostic surgical pathology,[49] confirming the outstanding *in vivo* anti-tumor effectiveness by utilizing the delivery of PTX in form of temperature sensitive β-CD-*g*-(PEG-*v*-PNIPAAm)$_7$/PTX supramolecular nanoparticles. In short, β-CD-*g*-(PEG-*v*-PNIPAAm)$_7$ with the ability to encapsulate PTX by supramolecular self-assembly and to form nanoparticles at body temperature could effectively inhibit the growth the drug resistant cancer cells, indicating their great potential in drug resistant cancer therapy.

4. Conclusions

In conclusion, a novel thermo-sensitive star polymer β-CD-*g*-(PEG-*v*-PNIPAAm)$_7$ with "V"-shaped arms is designed to encapsulate chemotherapeutic PTX or DOX through inclusion complex between β-CD host cavity and guest anti-cancer drug. At body temperature (above LCST), the phase transition of PNIPAAm chains anchored at the junction point of the "V"-shaped arms could facilitate the polymer-drug complex associate into stable supramolecular nanoparticle formation, which greatly enhanced the cellular endocytosis and intracellular drug retention, and further resulted in impairing MDR1 membrane pump mediated drug resistance. More importantly, both *in vitro* and *in vivo* results exhibited higher therapeutic efficacy of β-CD-*g*-(PEG-*v*-PNIPAAm)$_7$/drug supramolecular nanoparticles than the commercial formulation of drugs in overcoming pump mediated drug resistance. All these positive results signify that thermo-sensitive supramolecular chemotherapy is promising in conquering drug resistant tumor therapy and may serve as a new platform to design advanced drug delivery carriers to combat resistant cancer.

Supporting Information

Supporting Information is available from the Wiley Online Library.

Acknowledgements: The authors would like to thank the support by the Natural Science Foundation of China (81773661, U1504214, 21303145) and the Fundamental Research Funds for the Central Universities (20720170066), and express gratitude to the A*STAR Grant for support of this project.

5. Reference

[1] G. L. Beretta, F. Cavalieri, *Curr. Med. Chem.* **2016**, *23*, 3.

[2] Y. Liu, Q. Li, L. Zhou, N. Xie, E. C. Nice, H. Zhang, C. Huang, Y. Lei, *Oncotarget.* **2016**, *7*, 42740.

[3] C. Holohan, S. Van Schaeybroeck, D. B. Longley, P. G. Johnston, *Nat. Rev. Cancer.* **2013**, *13*, 714.

[4] P. Cai, W. R. Leow, X. Wang, Y.-L. Wu, X. Chen, *Adv. Mater.* **2017**, *29*, 1605529.

[5] B. E. Jeong, E. J. Ko, H. G. Joo, *Food. Chem. Toxicol.* **2012**, *50*, 1480.

[6] K. Tomoda, Y. T. Tam, H. Cho, D. Buehler, K. R. Kozak, G. S. Kwon, *Macromol. Biosci.* **2017**, *17*, 1600194.

[7] X. Fan, S. Jiang, Z. Li, X. J. Loh, *Mater. Sci. Eng. C.* **2017**, *73*, 275.

[8] B. Y. Ong, S. H. Ranganath, L. Y. Lee, F. Lu, H. S. Lee, N. V. Sahinidis, C. H. Wang, *Biomaterials.* **2009**, *30*, 3189.

[9] Y. Xiang, N. N. L. Oo, J. P. Lee, Z. Li, X. J. Loh, *Drug Discovery Today*. **2017**, *22*, 1318.

[10] D. P. Yang, M. Oo, G. R. Deen, Z. Li, X. J. Loh, *Macromol. Rapid Commun.* **2017**, 1700410.

[11] X. Fan, Z. Li, X. J. Loh, *Polym. Chem.* **2016**, *7*, 5898.

[12] P. Singh, K. Rathinasamy, R. Mohan, D. Panda, *IUBMB life.* **2008**, *60*, 368.

[13] Y.-L. Wu, H. Wang, Y.-K. Qiu, S. S. Liow, Z. Li, X. J. Loh, *Adv. Healthcare Mater.* **2016**, *5*, 2679.

[14] A. K. Singla, A. Garg, D. Aggarwal, *Int. J. Pharm.* **2002**, *235*, 179.

[15] Y. Gu, *Mater. Sci. Eng. C.* **2017**, *70*, 572.

[16] C. Chun, S. M. Lee, S. Y. Kim, H. K. Yang, S. C. Song, *Biomaterials.* **2009**, *30*, 2349.

[17] T. Wang, X. Tang, J. Han, Y. Ding, W. Guo, M. Pei, *Macromol. Biosci.* **2016**, *16*, 774.

[18] S. S. Liow, Q. Dou, D. Kai, Z. Li, S. Sugiarto, C. Y. Y. Yu, R. T. K. Kwok, X. Chen, Y. L. Wu, S. T. Ong, *Small.* **2017**, *13*, 1603404.

[19] A. A. Karim, Q. Dou, Z. Li, X. J. Loh, *Chem. - Asian J.* **2016**, *11*, 1300.

[20] Z. Li, H. Yin, Z. Zhang, K. L. Liu, J. Li, *Biomacromolecules.* **2012**, *13*, 3162.

[21] X. Fan, X. Wang, M. Cao, C. Wang, Z. Hu, Y.-L. Wu, Z. Li, X. J. Loh, *Polym. Chem.* **2017**, *8*, 5611.

[22] Y.-L. Wu, H. Yin, F. Zhao, J. Li, *Adv. Healthcare Mater.* **2013**, *2*, 297.

[23] Y.-L. Wu, J. Li, *Angew. Chem. Int. Ed.* **2009**, *48*, 3842.

[24] O. Swiech, A. Mieczkowska, K. Chmurski, R. Bilewicz, *J. Phys. Chem. B.* **2012**, *116*, 1765.

[25] J. J. Nie, X. B. Dou, H. Hu, B. Yu, D. F. Chen, R. X. Wang, F. Xu, *ACS Appl. Mater. Interfaces.* **2015**, *7*, 553.

[26] Y. Y. Yang, H. Hu, X. Wang, F. Yang, H. Shen, F. J. Xu, D. C. Wu, *ACS Appl. Mater. Interfaces.* **2015**, *7*, 12238.

[27] X. Fan, X. Wang, M. Cao, C. Wang, Z. Hu, Y.-L. Wu, Z. Li, X. J. Loh, *Polym. Chem.* **2017**, *8*, 5611.

[28] X. Chen, Y.-K. Qiu, C. Owh, X. J. Loh, Y.-L. Wu, *Nanoscale.* **2016**, *8*, 18876.

[29] E. Ye, P. L. Chee, A. Prasad, X. Fang, C. Owh, V. J. J. Yeo, X. J. Loh, *Mater. Today.* **2014**, *17*, 194.

[30] X. J. Loh, *Mater. Horiz.* **2014**, *1*, 185.

[31] Y. Lee, R. Graeser, F. Kratz, K. E. Geckeler, *Adv. Funct. Mater.* **2011**, *21*, 4211.

[32] L. Wang, X. Lin, J. Wang, Z. Hu, Y. Ji, S. Hou, Y. Zhao, X. Wu, C. Chen, *Adv. Funct. Mater.* **2014**, *24*, 4229.

[33] P. Zhao, W. Yin, A. Wu, Y. Tang, J. Wang, Z. Pan, T. Lin, M. Zhang, B. Chen, Y. Duan, *Adv. Funct. Mater.* **2017**, 1700403.

[34] X. Wei, Y. Wang, X. Xiong, X. Guo, L. Zhang, X. Zhang, S. Zhou, *Adv. Funct. Mater.* **2016**, *26*, 8266.

[35] X. Fan, M. Cao, X. Zhang, Z. Li, *Mater. Sci. Eng. C.* **2017**, *76*, 211.

[36] V. Dimitris, F. George, P. Tadeusz, R. Jacques, *J. Phys.: Condens. Matter.* **2001**, *13*, R855.

[37] Z. Li, D. Yuan, G. Jin, B. H. Tan, C. He, *ACS Appl. Mater. Interfaces.* **2016**, *8*, 1842.

[38] J. Li, X. J. Loh, *Adv. Drug Delivery Rev.* **2008**, *60*, 1000.

[39] S. Xia, Y. Wen, J. L. Zhu, Z. Feng, Z. Zhang, J. Li, *Biomacromolecules.* **2016**, *17*, 3957.

[40] A. Alomar, S. Abdou, R. L. De, A. Marsura, C. Finance, *Bioorg. Med. Chem. Lett.* **1999**, *9*, 1115.

[41] C. Yi, X. H. Pang, C. M. Dong, *Adv. Funct. Mater.* **2010**, *20*, 579.

[42] L. Sun, W. Liu, C. M. Dong, *Chem. Commun.* **2011**, *47*, 11282.

[43] C. Ding, Z. Li, *Mater. Sci. Eng. C.* **2017**, *76*, 1440.

[44] X. Fan, W. Zhang, Z. Hu, Z. Li, *J. Mater. Chem. B.* **2017**, *5*, 1062.

[45] B. H. Jeong, K. Jeon, H. Y. Park, O. J. Kwon, K. S. Lee, H. K. Kim, Y. S. Choi, J. Kim, H. J. Huh, N. Y. Lee, W. J. Koh, *J. Antimicrob. Chemother.* **2015**, *70*, 3127.

[46] K. A, T. Y, R. XQ, M. H, M. S, A. S, P. Y, *Mol. Cancer Ther.* **2002**, *1*, 1327.

[47] H. Cheng, Z. Wu, C. Wu, X. Wang, S. S. Liow, Z. Li, Y.-L. Wu, *Mater. Sci. Eng. C.* **2017**, DOI: 10.1016/j.msec.2017.08.075.

[48] F. Kong, X. Zhang, H. Zhang, X. Qu, D. Chen, M. Servos, E. Mäkilä, J. Salonen, H. A. Santos, M. Hai, *Adv. Funct. Mater.* **2015**, *25*, 3330.

[49] D. C. Brown, K. C. Gatter, *Histopathol.* **2002**, *40*, 2.

The table of contents entry. Thermo-sensitive supramolecular chemotherapy from β-CD-*g*-(PEG-*v*-PNIPAAm)$_7$ star polymer exhibited high potential in conquering drug resistant cancers.

Keywords: supramolecular chemotherapy, drug resistance, host-guest, thermo-sensitive

By Xiaoshan Fan[†], Hongwei Cheng [†], Xiaoyuan Wang, Enyi Ye, Xian Jun Loh, Yun-Long Wu*, Zibiao Li*

Thermo-responsive Supramolecular Chemotherapy by "V"-shape Armed β-Cyclodextrin Star Polymer to Overcome Drug Resistance

Table of Contents (TOC)

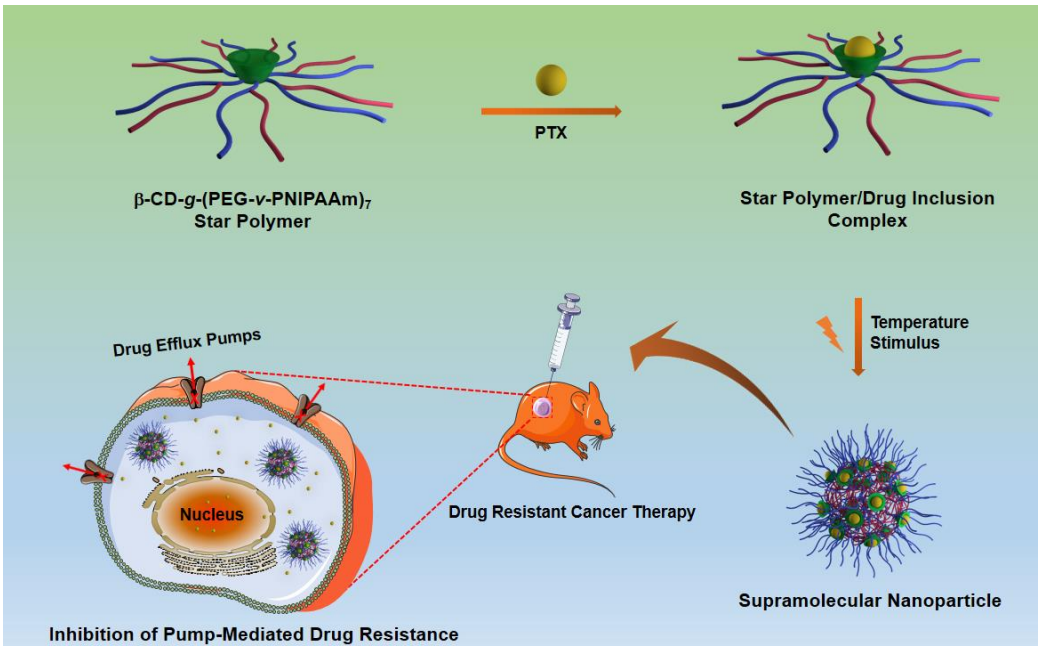

Thermo-sensitive supramolecular chemotherapy from β-CD-*g*-(PEG-*v*-PNIPAAm)$_7$ star polymer exhibited high potential in conquering drug resistant cancers